

AD-781 526

INTERACTION OF RADIATION AND MATTER

Amnon Yariv

California Institute of Technology

Prepared for:

Army Research Office-Durham
Advanced Research Projects Agency

31 December 1972

DISTRIBUTED BY:

NTIS

National Technical Information Service
U. S. DEPARTMENT OF COMMERCE
5285 Port Royal Road, Springfield Va. 22151

ARO-10242 10-7

California Institute of Technology
Pasadena, California 91109

FINAL REPORT
INTERACTION OF RADIATION AND MATTER
Contract DA-ARO-D-31-124-72-G86
1 January 1972 - 31 December 1972

Sponsored by the
Advanced Research Projects Agency
ARPA Order No. 675

Monitored by
Army Research Office
(Dr. R. Lontz)

Principal Investigator:

Amnon Yariv
(213) 795-6811
Ext. 1826

Reproduced by
NATIONAL TECHNICAL
INFORMATION SERVICE
U. S. Department of Commerce
Springfield VA 22161

AD781526

TECHNICAL DISCUSSION

I. High Gain Lasers

During the year 1972 we concluded our work on high gain lasers.

The work consisted of theoretical and experimental investigation of spectral, temporal and modal properties of extremely high gain lasers. The experiments were conducted using xenon 3.51 μm lasers with gains up to 60 db/m.

A number of significant effects were predicted by the theory and checked in experiments. A number of resulting publications (see References 1 and 2) the the Ph.D. thesis of Dr. L. Casperson summarize the results.⁶

II. Nonlinear Optics

Accurate measurements were performed to determine the nonlinear optical properties of a number of important materials. These include KDP, RDP, RDA, and LiIO_3 . The results are described in the enclosed Reference 3.

A theoretical analysis was carried out which points out a new technique for phase matching in nonlinear optical interactions. The technique involves fine corrugation of thin dielectric waveguides. Details are presented in Reference 4.

III. Optical Damage

Working with C. Giuliano of the Hughes Research Laboratories, it was shown experimentally and theoretically that the use of an elliptical cross section Gaussian beam can lead to large increases in the self focusing damage threshold of laser materials.

This suggests the incorporation of astigmatic optics in high power laser systems (see Reference 5).

Gain and Dispersion Focusing in a High Gain Laser

Lee W. Casperson and Amnon Yariv

The transverse modes of a laser resonator containing a medium with a strong radial gain profile differ greatly from the modes of a similar resonator containing a low gain medium. Focusing and defocusing effects result from the gain profile and from the associated dispersion profile. The dispersion focusing causes an asymmetry in the power output as the laser is tuned across the gain line. The theory has been verified using a high gain 3.51- μ xenon laser.

I. Introduction

In lenslike media having an approximately quadratic radial variation of either the gain or the index of refraction there is a focusing or defocusing of propagating Gaussian beams.^{1,2} A positive index profile results in a spot size of an unmatched beam which oscillates periodically with distance, while a positive gain profile causes the beam to approach a steady-state spot size. In a high gain gas discharge there is often a strong profile of the gain, so that gain focusing is likely to be important. However, whenever a medium has a gain spectrum, it must also have an associated dispersion spectrum. Therefore, dispersion focusing effects must always accompany gain focusing. It is the purpose of this paper to show that the two types of focusing are comparable in importance and that, moreover, the dispersion focusing may lead to asymmetry in Lamb dip measurements. Ordinarily asymmetries in the output of simple gas lasers are attributed to collisions between the atoms.^{3,4} The lasers considered are assumed to be operated very near threshold, so that self-focusing is unimportant.⁵ This treatment is based on one given elsewhere.⁶

II. Theory

A lenslike medium is one in which the complex propagation constant k varies quadratically with radius according to

$$k = k_0 - \frac{1}{2}k_2 r^2. \quad (1)$$

The real and imaginary parts of k are given by

$$k = \beta + i\alpha. \quad (2)$$

Here α is the exponential gain constant for the electric field and β is related to the index of refraction by

$$\beta = 2\pi n/\lambda. \quad (3)$$

The easiest way to study the propagation of Gaussian beams through such lenslike media is in terms of the complex beam parameter q given by

$$1/q = (1/R) - i(\lambda_m/\pi w^2), \quad (4)$$

where R is the radius of curvature of the phase fronts, w is the spot size of the beam, and λ_m is the wavelength in the medium. The same beam parameter may also be used to characterize higher order Laguerre-Gaussian and Hermite-Gaussian beams.

From the wave equation one finds that the propagation of q is governed by the Ricatti equation¹

$$(1/q)^{\dagger} + (d/dz)(1/q) + (k_2/k_0) = 0. \quad (5)$$

For simplicity we assume here that saturation is unimportant and the coefficients k_0 and k_2 are independent of position along the axis of the medium. The solution of Eq. (5) is

$$1/q_1 = \{[(1/q_1) \cos(k_2/k_0)^{\dagger} z] - [(k_2/k_0)^{\dagger} \sin(k_2/k_0)^{\dagger} z] \} \\ + \{[(1/q_1)(k_0/k_2)^{\dagger} \sin(k_2/k_0)^{\dagger} z] + [\cos(k_2/k_0)^{\dagger} z]\}. \quad (6)$$

Except when $(k_2/k_0)^{\dagger}$ is real, the beam parameter at large distances approaches the limiting value

$$1/q_{\infty} = \mp i(k_2/k_0)^{\dagger}, \quad (7)$$

where the upper sign is used if $\text{Im}(k_2/k_0)^{\dagger} > 0$ and the lower sign is used if $\text{Im}(k_2/k_0)^{\dagger} < 0$.

In the special case $\text{Im}(k_2/k_0)^{\dagger} = 0$, $\text{Re}(k_2/k_0)^{\dagger} \neq 0$ (no gain profile), the beam parameter oscillates periodically without approaching a steady-state value. If $(k_2/k_0)^{\dagger} = 0$ so that there is no profile at all, Eq. (6) reduces to the free space result

$$q_1 = q_0 + z. \quad (8)$$

Otherwise, after some oscillation the beam goes to the limit given in Eq. (7). From Eqs. (4) and (7) the limit-

Both authors were with the Division of Engineering and Applied Science, California Institute of Technology, Pasadena, California 91109; L. W. Casperson is now with the UCLA School of Engineering and Applied Science.

Received 4 June 1971.

ing spot size is

$$w_\infty = (\lambda_m/\pi)^{1/2} [\pm \text{Re}(k_2/k_0)]^{-1/2} \quad (9)$$

and the limiting radius of curvature of the phase fronts is

$$R_\infty = [\pm \text{Im}(k_2/k_0)]^{-1}. \quad (10)$$

The spot size given by Eq. (9) must be real if the beam is to be confined by the medium. With our sign convention this means that the real and imaginary parts of $(k_2/k_0)^{1/2}$ must have the same sign, or that

$$\text{Im}(k_2/k_0) > 0. \quad (11)$$

With Eq. (2) this stability condition is simply

$$\alpha_2 > 0, \quad (12)$$

provided that the gain per wavelength is small ($\beta_0 \gg \alpha_0$). In other words, the gain profile causes a *damped focusing* such that the beam approaches a stable steady-state value if and only if the gain is highest on the axis of the medium. It is only this stable situation which is of interest in the remainder of this paper. From Eqs. (9) and (10) the spot size is

$$w_\infty = (\lambda_m/\pi)^{1/2} \{ \pm \text{Re}[(\beta_2 + i\alpha_2)/\beta_0] \}^{-1/2} \quad (13)$$

and the radius of curvature of the phase fronts is

$$R_\infty = \{ \pm \text{Im}[(\beta_2 + i\alpha_2)/\beta_0] \}^{-1}. \quad (14)$$

We have described so far the propagation of Gaussian beams in long high gain laser amplifiers. The transverse modes of a laser resonator containing a high gain medium are most easily found using complex beam matrices.² In the remainder of this paper we consider only the simplest type of high gain laser, which consists of a plane parallel resonator filled with a lenslike medium. Such a configuration can be well approximated in practice. The spot size everywhere in this laser is equal to the limiting value given by Eq. (13), which can be written as

$$w = \{ (\pi\alpha_2/4\lambda_m) \{ [1 + (\beta_2/\alpha_2)^2]^{1/2} + (\beta_2/\alpha_2) \} \}^{-1/2}. \quad (15)$$

This result can be applied to lasers with various types of index profiles. In the following, only profiles due to the gain and dispersion will be considered.

To find how the spot size in Eq. (15) depends on frequency, it is necessary to know the frequency dependence of α_2 and β_2 . In a Doppler-broadened medium the unsaturated intensity gain g is a Gaussian function of frequency and $\alpha_2(x)$ may be written

$$\alpha_2(x) = (g_2'/2)e^{-x^2}, \quad (16)$$

where $x = 2(\nu - \nu_0)(\ln 2)^{1/2}/\Delta\nu_D$ is a normalized frequency and g_2' is the line center value of the quadratic term in the intensity gain constant. The quadratic term in the index of refraction of a Doppler-broadened medium is⁷

$$n_2(x) = (\lambda g_2'/2\pi^{3/2})F(x), \quad (17)$$

where $F(x)$ is Dawson's integral given by

$$F(x) = e^{-x^2} \int_0^x e^{t^2} dt. \quad (18)$$

Therefore $\beta_2(x)$ is simply

$$\beta_2(x) = (g_2'/\pi^{3/2})F(x). \quad (19)$$

Using Eqs. (16) and (19) in Eq. (15), one obtains the following expression for the frequency-dependent spot size of a plane parallel gain-focused laser:

$$w(x) = \left[\frac{\pi g_2'}{8\lambda_m} e^{-x^2} \left(\left\{ 1 + \left[\frac{2F(x)e^{x^2}}{\pi^{1/2}} \right]^2 \right\}^{1/2} + \frac{2F(x)e^{x^2}}{\pi^{1/2}} \right) \right]^{-1/2} \quad (20)$$

It is convenient to define the normalized spot size $w^*(x)$ given by

$$w^*(x) = e^{x^2/4} \left(\left\{ 1 + \left[\frac{2F(x)e^{x^2}}{\pi^{1/2}} \right]^2 \right\}^{1/2} + \frac{2F(x)e^{x^2}}{\pi^{1/2}} \right)^{-1/2}, \quad (21)$$

which is equal to the actual spot size divided by its line center value. A plot of $w^*(x)$ is given in Fig. 1.

Fig. 1

Also plotted in the figure is the function $e^{x^2/4}$, which would represent the frequency dependence of the normalized spot size if dispersion focusing were neglected. The asymmetry of the spot size results from the positive and negative dispersion focusing, which occur, respectively, for positive and negative values of the frequency x . The minimum value of the spot size is at a frequency of about $x \approx 0.6$ rather than at line center.

We are primarily interested here in inhomogeneously broadened media, but the results for homogeneous broadening are similar. In an unsaturated homogeneous medium the gain is the Lorentzian

$$\alpha_2(y) = (g_2'/2)[1/(1 + y^2)], \quad (22)$$

where $y = 2(\nu - \nu_0)/\Delta\nu_n$ is a normalized frequency. The index of refraction is

$$n_2(y) = (\lambda g_2'/4\pi)[y/(1 + y^2)]. \quad (23)$$

Therefore, from Eq. (15) the spot size is given by

$$w = \{ (\pi g_2'/8\lambda_m) [1/(1 + y^2)] [(1 + y^2)^{1/2} + y] \}^{-1/2}. \quad (24)$$

These homogeneous results are not considered further.

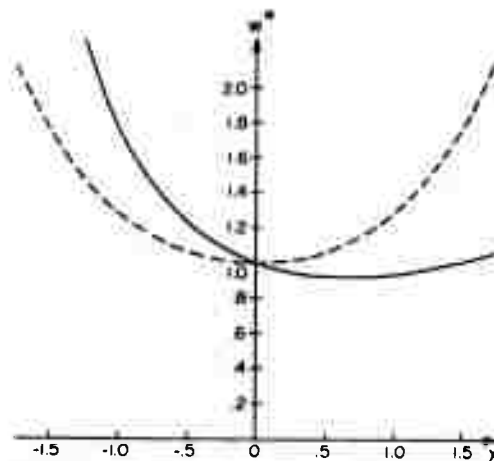


Fig. 1. Solid line is the normalized spot size as a function of frequency. Dashed line is the spot size neglecting dispersion focusing.

The difference between the spot sizes indicated by the two curves in Fig. 1 is at most of the order of 10%. Nevertheless, the dispersion focusing could, in principle, be detected directly by scanning the output beam profile of a laser if the oscillation frequency were known. A more important practical consequence of the dispersion focusing is that the total power output of the laser becomes asymmetric about line center. One expects that for equal values of the gain, the larger the beam spot size, the greater the output power. In particular, the maximum power output of the laser does not occur when the oscillation frequency is at gain center (neglecting the Lamb dip, of course). The asymmetry in the power output is easily measured and provides a fairly direct indication of dispersion focusing.

The growth of intensity in a saturating one-dimensional inhomogeneously broadened laser is governed by the well-known expression

$$dI/dz = gI/(1 + sI)^{1/2}, \quad (25)$$

where s is a saturation parameter. For simplicity distributed losses are neglected. For very weak saturation ($sI \ll 1$) Eq. (25) reduces to the homogeneous approximation

$$dI/dz = gI/(1 + \frac{1}{2}sI). \quad (26)$$

If the laser beam were uniform over an area of radius w and there were no gain profile, then the corresponding result for the growth of the total power would be

$$dP/dz = g_0P/[1 + \frac{1}{2}(sP/\pi w^2)]. \quad (27)$$

Equation (27) can be shown to be also valid for a Gaussian beam with nearly plane phase fronts in a medium with a quadratic gain profile, provided that the square of the spot size w is much smaller than the square of the discharge diameter r_0 .⁶ This is not always a good approximation but it is valid for our experiments. g_0 is the unsaturated gain at the axis of the medium. The result for a homogeneously broadened medium would be the same as Eq. (27) except that the factor $\frac{1}{2}$ would be missing.

If one mirror is highly reflecting, Eq. (27) can be integrated for one loop through the laser medium, and the result is

$$\frac{1}{2}(s/\pi w^2)(P_2 - P_1) = 2g_0l - \ln(P_2/P_1), \quad (28)$$

where l is the length of the medium. This integration is possible as long as the right and left traveling beams interact with different velocity classes of atoms. If the reflectivity of the output mirror is R and the transmission is T , then Eq. (28) may be solved for the output power P_0 as

$$P_0 = (2\pi w^2/s)[T/(1 - R)](2g_0l + \ln R). \quad (29)$$

A similar result can be obtained for homogeneously broadened lasers.

Using Eq. (20) for the frequency-dependent spot size with $g_0 = g_0' e^{-x^2}$, one obtains finally

$$P_0(x) = (4r_0/s)(\pi\lambda_m/1.44g_0')^{1/2} e^{x^2/2} [T/(1 - R)] (2g_0' l e^{-x^2} + \ln R) \times \{ [1 + [2F(x)e^{x^2}/\pi^{1/2}]^2]^{1/2} + [2F(x)e^{x^2}/\pi^{1/2}] \}^{-1/2}. \quad (30)$$

We have assumed here that the medium has a Bessel function radial gain profile, so that the quadratic term is²

$$g_1 = g_0(2.88/r_0^2). \quad (31)$$

Equation (30) is the general expression for the frequency dependence of the output power of a Doppler-broadened laser oscillator (neglecting the Lamb dip). The exact calculation of the Lamb dip is difficult in high gain lasers. However, as long as the homogeneous line width is small compared to the Doppler line width, the Lamb dip provides a useful indication of line center ($x = 0$) without significantly affecting the over-all line shape.

It is convenient to define the normalized power spectrum

$$P_0^*(x) = (e^{-x^2} - b)e^{x^2/2} \{ [1 + [2F(x)e^{x^2}/\pi^{1/2}]^2]^{1/2} + [2F(x)e^{x^2}/\pi^{1/2}] \}^{-1/2}, \quad (32)$$

where

$$b = -(\ln R/2g_0'l) \quad (33)$$

is a threshold parameter which is less than unity if the laser is saturated. Equation (32) is plotted in Fig. 2 for various values of the parameter b . Evidently when the laser is above threshold, the greatest output occurs at a slightly negative frequency rather than at line center. Near threshold ($b \rightarrow 1$) this effect diminishes and the greatest output occurs near $x = 0$. Also plotted in Fig. 2 is the gain spectrum e^{-x^2} .

The asymmetry of the power spectrum is most conveniently characterized by the location in frequency of the power maximum. In Fig. 5 is a plot of this frequency as a function of the threshold parameter b . The plots in Figs. 2 and 5 are not quantitatively correct for all values of b . From Eqs. (27) and (29) this homogeneous approximation is only valid in an inhomogeneously broadened medium as long as the product $(2g_0l + \ln R)(1 - R)^{-1}$ is small compared to unity. In a

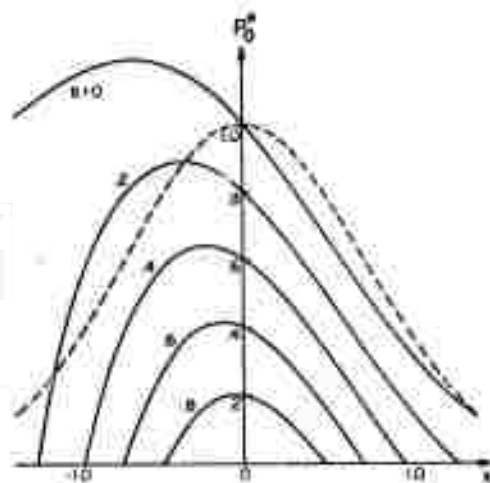


Fig. 2. Normalized power output as a function of frequency for various values of the threshold parameter. Dashed line is the gain spectrum.

high loss laser ($R \ll 1$) this is the same as requiring that b be nearly equal to unity. Nevertheless, these results are expected to be qualitatively correct for most values of b .

It is possible to obtain a simpler approximate expression for the output power as a function of frequency which is valid for small values of x . One finds after some algebra that Eq. (32) may be expanded to second order in x as

$$P_o^*(x) \simeq (1 - b) - [(1 - b)/\pi^2]x + \{[(1 - b)/2\pi] - [(1 + b)/2]\}x^2. \quad (34)$$

The maximum of this spectrum occurs at the frequency

$$x_{\max} = \{\pi^{-1} - [(1 + b)/(1 - b)]\pi^2\}^{-1}. \quad (35)$$

If b is nearly equal to unity, then the maximum is at

$$x_{\max} = -[(1 - b)/2\pi^2]. \quad (36)$$

This equation is plotted as a dashed line in Fig. 5. The two lines in the figure are in good agreement in the limit of weak saturation.

In this section we have discussed focusing effects which are due to the gain and dispersion profiles which

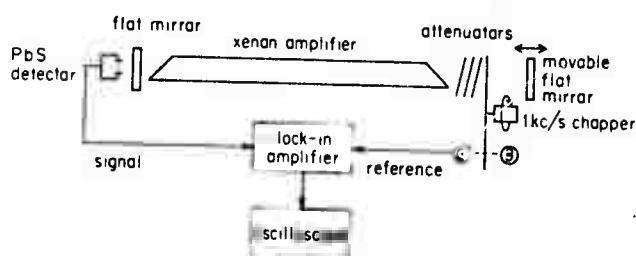


Fig. 3. Experimental setup.

may be associated with a high gain laser transition. It was shown that the spot size of a waveguided beam is greater for frequencies below gain center than for frequencies greater than gain center. As a consequence of this focusing asymmetry, the power output maximum occurs at a frequency slightly below gain center. Experimental verification of the theory is described in the next section.

III. Experiment

The gain focusing and dispersion focusing have been observed experimentally using a high gain 3.51- μ xenon laser. In a discharge laser of this type the gain maximum must be at the axis of the discharge with the gain falling to zero at the tube walls. This gain profile makes the xenon laser appropriate for studying focusing effects.

The spot size in a simple plane parallel resonator filled with an unsaturated high gain medium is given by Eq. (20). For frequencies near line center Dawson's integral $F(x)$ goes to zero and the spot size is simply

$$w(x) = (8\lambda_m/\pi q_2)^{1/2}. \quad (37)$$

Experimental investigations of this result have been reported previously.² The purpose of this section is to consider experimentally the more subtle frequency asymmetry resulting from dispersion focusing.

The apparatus is shown in Fig. 3. The dc discharge was about 5.5 mm in diameter and 1.1 m in length. The right mirror was highly reflecting and could be translated longitudinally by means of a motor drive. The cavity length was 1.29 m, so the empty cavity mode spacing would be about $c/2L = 116$ MHz. Synchronous detection was used to improve the signal-to-noise ratio, and monoisotopic xenon was used to prevent unnecessary asymmetries in the output. The xenon pressure was maintained at about 5 μ by means of a liquid nitrogen trap.⁸

A typical plot of the power output for decreasing cavity length (increasing frequency) is shown in Fig. 4. The laser was operated very near threshold and the peaks represent successive longitudinal modes. These peaks are to be compared to the theoretical curves shown in Fig. 2. In the experimental plot there is a dip in the output power on the high frequency side of the peak. This is the Lamb dip and it results from the interaction of the left and right traveling beams with atoms which have zero z -component of velocity. Thus the Lamb dip provides a convenient indication of the frequency $x = 0$.

Comparison of the experimental and theoretical plots shows that the power maximum is shifted down in frequency by roughly the amount predicted by the dispersion focusing theory. Some data are shown in Fig. 5. The value of the gain as a function of discharge current was determined by introducing known losses into the cavity and reducing the current until threshold was reached. The reflectivity of the output mirror was 4% and the value of b is given by Eq. (33). For the analysis of the data it was necessary to take into account mode pulling, because with a dispersive medium of this sort the rate of change of the frequency with mirror position may be greatly reduced near line center.⁹ For a rigorous comparison of the experimental and theoretical results over the entire spectrum it would have been necessary to include the nonlinear mode pulling which occurs near the wings of the gain line. The pressure was low enough in these experiments that collision effects are believed to be completely unimportant. The experiments indicate that the threshold Lamb dip in xenon has a width of about 6 ± 1 MHz and a depth somewhat greater than the 10% enhanced Lamb dip reported previously.¹⁰

A possible cause of asymmetry in the power measurements is the mass motion of the emitting atoms.¹¹ Particularly in a low pressure dc discharge one might expect a drift of the ions toward the cathode compensated by a drift of neutral atoms toward the anode. In a high gain laser the Doppler shifts resulting from this mass motion would result in an asymmetry of the output power spectrum. However, the asymmetry for light emerging from one end of the laser would be expected to be in the opposite direction to the asymmetry for light emerging from the other end. To check this

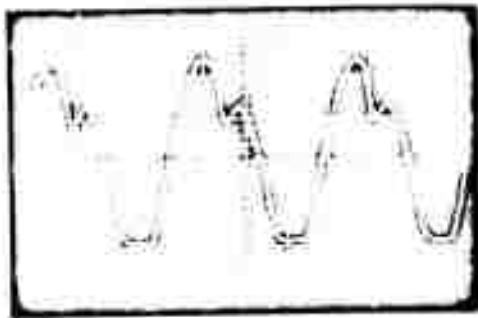


Fig. 4. Power output for decreasing cavity length with a discharge current of 18 mA.

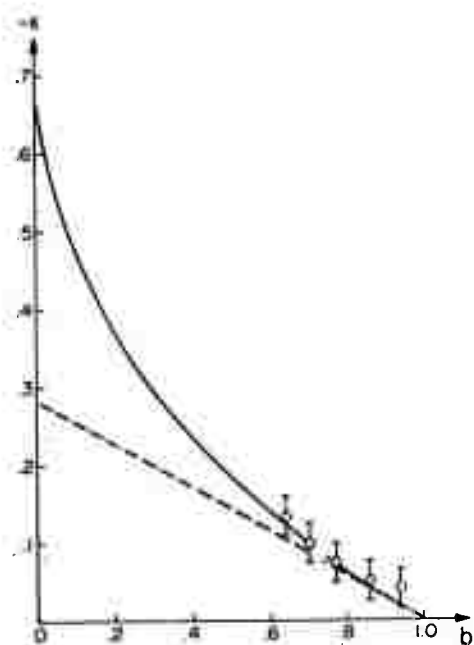


Fig. 5. Frequency of the power maximum vs the threshold parameter b . The solid line is a theoretical result obtained from Eq. (32) and the dashed line is a plot of Eq. (36). The circles are experimental values.

possibility a resonator was constructed having equally transmitting mirrors at the two ends. It was found that the power spectrum was identical at the two ends of the laser, indicating that for the conditions of our experiments drift of the atoms is unimportant. The shift resulting from the known abundances of impurity isotopes is estimated to be small compared to the observed asymmetry.

IV. Conclusion

The transverse modes of a laser containing a high gain medium may differ significantly from the modes of a similar low gain laser because of gain and dispersion focusing. The dispersion effects result in an asymmetry of the output power spectrum which could be important in any Lamb dip measurements in lasers with moderately high gain. Experiments with a high gain 3.51- μ xenon laser have yielded results in agreement with the theory. While only plane parallel resonators have been considered here, the results may readily be extended to more complicated laser configurations.

This research was supported by the Advanced Research Projects Agency through the Army Research Office, and by the Air Force Office of Scientific Research.

References

1. H. Kogelnik, *Appl. Opt.* **4**, 1562 (1965).
2. L. W. Casperson and A. Yariv, *Appl. Phys. Lett.* **12**, 355 (1968).
3. A. Szöke and A. Javan, *Phys. Rev.* **145**, 137 (1966).
4. B. L. Gyorffy, M. Borenstein, and W. E. Lamb, Jr., *Phys. Rev.* **169**, 340 (1968).
5. A. Javan and P. L. Kelley, *IEEE J. Quant. Electron.* **QE-2**, 470 (1966).
6. L. W. Casperson, Ph.D. thesis, California Institute of Technology (1971), Chap. 5.
7. D. H. Close, *Phys. Rev.* **153**, 360 (1967), Eq. (44).
8. D. R. Armstrong, *IEEE J. Quant. Electron.* **QE-4**, 968 (1968).
9. L. W. Casperson and A. Yariv, *Appl. Phys. Lett.* **17**, 259 (1970).
10. S. C. Wang, R. L. Byer, and A. E. Siegman, *Appl. Phys. Lett.* **17**, 120 (1970).
11. A. D. White, *Appl. Phys. Lett.* **10**, 24 (1967).

Spectral Narrowing in High-Gain Lasers

LEE W. CASPERSON AND AMNON YARIV, FELLOW, IEEE

Abstract—The dependence of spectral narrowing in lasers on the line-broadening mechanism is investigated including the effects of saturation and distributed loss. It is found that in the unsaturated regime the narrowing is essentially independent of the resonance broadening mechanism and the narrowed line approaches a Gaussian. The onset of saturation slows or reverses the narrowing process. Experimental results have been obtained using a 3.51- μ xenon laser.

I. INTRODUCTION

SPECTRAL narrowing refers to the fact that under some circumstances radiation incident on a laser amplifier or generated within an amplifier will emerge with a spectrum which is narrower than the one it started with [1]. In high-gain lasers spectral narrowing may be substantial and can provide a highly stable and monochromatic light source. The applications of such optical frequency standards in metrology are well known [2]. Comparison of the input and output spectra of a laser amplifier might provide a sensitive indirect measurement of the amplifier gain.

The purpose of this paper is to study in some detail the influence of an amplifying medium on a spectral continuum including the effects of saturation and distributed loss. Emphasis is placed on the important problem of superradiance, but narrowing in other amplifiers is also considered and limiting line widths are determined.

The starting point for this investigation is a general expression for the incremental gain of a monochromatic signal in a laser amplifier. From the derivation of Gordon *et al.* [3] the intensity of radiation at the frequency ν_i in a Doppler broadened medium is described by

$$\frac{dI_i}{dz} = \frac{kI_i}{\pi} \int_{-\infty}^{\infty} \frac{\exp(-\epsilon^2 y^2)}{[1 + (y - y_i)^2] \left[1 + \frac{sI_i}{1 + (y - y_i)^2} \right]} dy \quad (1)$$

where $y(\nu) = 2(\nu - \nu_0)/\Delta\nu_k$ is a normalized frequency, k is a pumping constant, s is a saturation parameter, and the natural damping ratio $\epsilon = (\Delta\nu_k/\Delta\nu_D)\sqrt{\ln 2}$ measures the relative importance of homogeneous and

Doppler broadening. The homogeneous and Doppler line widths are given respectively by $\Delta\nu_k$ and $\Delta\nu_D$. The derivation can be generalized in a straightforward fashion to the interaction with an optical continuum and the result is

$$\frac{dI(y_i)}{dz} = \frac{kI(y_i)}{\pi} \int_{-\infty}^{\infty} \frac{\exp(-\epsilon^2 y^2)}{[1 + (y - y_i)^2] \left[1 + s \int_{-\infty}^{\infty} \frac{I(y_n) dy_n}{1 + (y - y_n)^2} \right]} dy \quad (2)$$

where $I(y_i)$ is the spectral density at the frequency y_i . This result neglects any coherent interaction between the frequency components of the spectrum. However, it is found in practice that even with monochromatic fields coherence effects are usually unimportant [4] and the neglect of coherence makes possible a number of useful analytic solutions. Also, the extreme saturation that is necessary for coherence effects is generally found to impede the narrowing process, so that in any practical situation strong saturation would be avoided.

II. UNSATURATED AMPLIFIERS

In an unsaturated amplifier the growth of an intensity continuum is governed by

$$\frac{dI(y_i, z)}{dz} = g(y_i)I(y_i, z) - \alpha I(y_i, z) + \eta g(y_i). \quad (3)$$

The unsaturated incremental gain spectrum $g(y_i)$ is, for simplicity, assumed to be independent of the distance z . The second term on the right side of (3) represents distributed losses. The last term is the spontaneous emission, which has the same frequency dependence $g(y_i)$ as the incremental gain. This one-dimensional model is approximately valid in narrow bore amplifiers having a length much greater than the diameter. The coefficient η is then proportional to the spontaneous emission rate and to a geometrical factor that depends on the amplifier dimensions. A more rigorous three-dimensional treatment would have to account for the spatial distribution of the emitting atoms [5], the strong focusing effects that are common in high-gain lasers [6], and reflections at the boundaries of the amplifying medium. Solving for an amplifier of length z yields

$$I(y_i, z) = I(y_i, 0) \exp [(g(y_i) - \alpha)z] + \frac{\eta g(y_i)}{g(y_i) - \alpha} (\exp [(g(y_i) - \alpha)z] - 1). \quad (4)$$

Superradiance will be considered first. In a superradiant source there is no input and if losses are negli-

Manuscript received August 17, 1971; revised October 1, 1971. This work was supported in part by the Advanced Research Projects Agency through the Army Research Office, Durham, and in part by the Air Force Office of Scientific Research. This paper is based on part of a dissertation submitted by L. W. Casperson to the California Institute of Technology, Pasadena, in partial fulfillment of the requirements for the Ph.D. degree.

L. W. Casperson was with the California Institute of Technology, Pasadena, Calif. He is now with the School of Engineering and Applied Science, University of California, Los Angeles, Calif. 90024.

A. Yariv is with the California Institute of Technology, Pasadena, Calif. 91109.

gible (4) simplifies to

$$I(y_l, z) = \eta(\exp[g(y_l)z] - 1). \quad (5)$$

Defining $f(y_l)$ as the fraction of the line center intensity at the frequency y_l yields

$$f(y_l, z) = \frac{I(y_l, z)}{I(0, z)} = \frac{\exp[g(y_l)z] - 1}{\exp[g(0)z] - 1}. \quad (6)$$

Most lasers can be classed as either homogeneously or inhomogeneously broadened and only these cases will be considered here.

For homogeneous broadening ($\epsilon \gg 1$) and no saturation the gain from (2) is simply the Lorentzian

$$g(y_l)_{\text{hom}} = \frac{k}{\sqrt{\pi} \epsilon} \frac{1}{1 + y_l^2}. \quad (7)$$

The spectral width, defined as the separation between the two frequencies at which the spectral intensity is down to $\frac{1}{2}$ its peak value, is obtained by combining (7) with (6) for $f = \frac{1}{2}$. The result is

$$\Delta\nu_{\text{hom}} = \Delta\nu_h \sqrt{\frac{kz}{\sqrt{\pi} \epsilon} \ln \frac{1}{\frac{1}{2}(\exp[kz/\sqrt{\pi} \epsilon] + 1)} - 1}. \quad (8)$$

For short distances ($kz/\sqrt{\pi} \epsilon \ll 1$) the line width given by (8) is just the homogeneous line width $\Delta\nu_h$. For long distances ($kz/\sqrt{\pi} \epsilon \gg 1$) (8) simplifies to

$$\Delta\nu_{\text{hom}} \simeq \Delta\nu_h \sqrt{\frac{\sqrt{\pi} \epsilon}{kz} \ln 2} = \Delta\nu_h \sqrt{\frac{\ln 2}{g(0)_{\text{hom}} z}}. \quad (9)$$

Thus the narrowing effect becomes important when the product $g(0)_{\text{hom}} z$ becomes comparable to unity. The approximate result given by (9) becomes valid after the width is narrowed to about one half of its initial value.

For an unsaturated inhomogeneously broadened amplifier ($\epsilon \ll 1$) and for radiation not too far in the wings of the line ($y_l \ll 1/2 \epsilon^2$) the gain from (2) is the Gaussian

$$g(y_l)_{\text{inhom}} = k \exp(-\epsilon^2 y_l^2). \quad (10)$$

Combining this with (6) for $f = \frac{1}{2}$ yields

$$\Delta\nu_{\text{inhom}} = \Delta\nu_D \sqrt{\frac{\ln kz - \ln \ln \frac{1}{2}[\exp(kz) + 1]}{\ln 2}}. \quad (11)$$

For short distance ($kz \ll 1$) the width of the emission is equal to the Doppler width $\Delta\nu_D$. For long distances ($kz \gg 1$) one finds

$$\Delta\nu_{\text{inhom}} \simeq \Delta\nu_D \frac{1}{\sqrt{kz}} = \frac{\Delta\nu_D}{\sqrt{g(0)_{\text{inhom}} z}}. \quad (12)$$

These results suggest that the narrowing proceeds in about the same fashion independent of the line broadening mechanisms. To verify this conclusion, one may consider a completely general incremental gain function $g(y_l)$ with a maximum at the frequency $y_0 = 0$. Assuming that $g(y_l)$ is differentiable in the neighborhood of

zero, it may be expanded as

$$g(y_l) = g_0 - g_2 y_l^2 + g_3 y_l^3 + g_4 y_l^4 + \dots \quad (13)$$

where g_0 and g_2 are positive. The spectrum of the superradiance is given by (6) as

$$\begin{aligned} f(y_l) &= \frac{\exp[(g_0 - g_2 y_l^2 + g_3 y_l^3 + \dots)z] - 1}{\exp[g_0 z] - 1} \\ &= \frac{\exp[g_0 z] \exp\left[-\left(\frac{y_l}{\Delta_2}\right)^2\right] \exp\left[\left(\frac{y_l}{\Delta_3}\right)^3\right] \exp[(\dots)] - 1}{\exp[g_0 z] - 1} \end{aligned} \quad (14)$$

where $\Delta_n = (zg_n)^{-1/n}$.

At large distances ($g_0 z \gg 1$) the zero-order terms cancel, leaving

$$f(y_l) \simeq \exp\left[-\left(\frac{y_l}{\Delta_2}\right)^2\right] \exp\left[\left(\frac{y_l}{\Delta_3}\right)^3\right] \exp[(\dots)] \dots \quad (15)$$

Also, at very large distances one finds that $\Delta_n \ll \Delta_{n+1}$ so that the Gaussian factor is much narrower than the others. Consequently, all of the factors but the first may be replaced with their value at line center. Therefore,

$$f(y_l) \simeq \exp\left[-\left(\frac{y_l}{\Delta_2}\right)^2\right], \quad \Delta_2 = \frac{1}{\sqrt{g_2 z}}. \quad (16)$$

This is in agreement with the previous results for homogeneous and inhomogeneous broadening as may be verified by expanding $g(y_l)$ of (7) and (10) in power series in y_l to obtain g_2 . More generally if the incremental gain has several maxima, the emission will eventually resolve itself into narrowing Gaussian lines centered on the gain maxima. This resolving effect has been observed by Parks *et al.* [7].

So far only superradiance has been considered. If an amplifier has an input $I(y_l, 0)$ and negligible spontaneous emission, (6) for the output light spectrum is replaced by

$$F(y_l, z) = \frac{I(y_l, 0) \exp[g(y_l)z]}{I(0, 0) \exp[g(0)z]}. \quad (17)$$

At large distances this becomes

$$F(y_l, z) \simeq \frac{I(y_l, 0)}{I(0, 0)} \exp\left[-\left(\frac{y_l}{\Delta_2}\right)^2\right], \quad \Delta_2 = \frac{1}{\sqrt{g_2 z}}. \quad (18)$$

If the input is reasonably smooth the output spectrum is simply

$$F(y_l, z) \simeq \exp\left[-\left(\frac{y_l}{\Delta_2}\right)^2\right]. \quad (19)$$

If the input is a narrow Gaussian of width Δ_{in} , the output will be a Gaussian of width Δ_{out} such that

$$\left(\frac{1}{\Delta_{\text{out}}}\right)^2 = \left(\frac{1}{\Delta_{\text{in}}}\right)^2 + \left(\frac{1}{\Delta_2}\right)^2. \quad (20)$$

The concept of gain narrowing is sometimes useful instead of spectral narrowing. The two are obviously

closely related. If one assumes that the input spectrum in (17) is white, then the intensity factors cancel and $F(y_i)$ is a general expression for the gain spectrum of an amplifier normalized to unity on line center. Expressions for the gain line width, for example, are then obtained by setting F equal to one half and solving (17) for $y_{1/2}$. For an inhomogeneously broadened amplifier the results may be made to conform with those of Hotz [8].

In summary, one may conclude that in an unsaturated amplifier the width of the amplified spectrum decreases with distance. The shape of the spectrum approaches a Gaussian as the effective part of the gain approaches a quadratic. As an example, in a helium-xenon discharge the gain may be 400 dB/m [5] or nearly $k = 100$ so that the spectrum of a superradiant source 1 m long would be narrowed according to (12) by a factor of ten provided saturation did not occur. The Doppler width of xenon at room temperature is about $\Delta\nu_D = 100$ MHz, so the narrowed radiation would have a width of about 10 MHz. Since the frequency of the $3.51\text{-}\mu$ transition is about 10^8 MHz, the light would be monochromatic to a part in 10^7 . Collimation in a long high-gain gas laser is taken care of by the gain profile of the medium itself [6] and there should not be much difficulty in constructing a gas discharge amplifier of arbitrary length. However, care is necessary to prevent saturation as will be shown in the next section.

III. SATURATION EFFECTS

The intensity of amplified spontaneous emission can easily reach the saturation level. When this happens the behavior of the spectrum becomes considerably more complicated and for a completely general treatment computer solutions are required. We present here analytic solutions for certain important limiting situations and also some general computer results.

For a homogeneously broadened amplifier all of the factors but the Gaussian may be removed from the integral in (2). The result of the integration is

$$\frac{dI(y_i)}{dz} = \frac{kI(y_i)}{\sqrt{\pi}\epsilon h(z)} \frac{1}{1 + y_i^2} \quad (21)$$

where

$$h(z) = 1 + s \int_{-\infty}^{\infty} \frac{I(y_n) dy_n}{1 + y_n^2} \quad (22)$$

and distributed losses are ignored. Thus the gain profile remains Lorentzian even with saturation, although its amplitude decreases. The quadratic term in the frequency expansion of the gain decreases in magnitude and hence a narrow Gaussian beam will continue to narrow, but at a reduced rate as saturation becomes important. Solving as before yields for large distances

$$\Delta\nu_{\text{hom}} = \Delta\nu_A \sqrt{\sqrt{\pi}\epsilon \ln 2 / k \int \frac{dz}{h(z)}} \quad (23)$$

To proceed, expressions for $h(z)$ must be obtained.

For an intensity spectrum that is narrow compared to $\Delta\nu_A$ (22) becomes

$$h(z) \simeq 1 + s \int_{-\infty}^{\infty} I(y_n) dy_n = 1 + sI_t \quad (24)$$

where I_t is the total intensity. Such a spectrum would be obtained, for example, at large distances ($g(0)_{\text{hom}} z \gg 1$) in a superradiant amplifier. To evaluate $h(z)$, it is first necessary to find expressions for I_t . In this approximation (21) may be integrated over frequency yielding

$$\frac{dI_t}{dz} = \frac{kI_t}{\sqrt{\pi}\epsilon(1 + sI_t)} \quad (25)$$

Thus in an unsaturated amplifier the intensity grows according to

$$I_t = I_{t0} \exp[kz/\sqrt{\pi}\epsilon] \quad (26)$$

while in a highly saturated amplifier the intensity is governed by

$$I_t = I_{t0} + \frac{kz}{\sqrt{\pi}\epsilon s} \quad (27)$$

The intensity in the saturated amplifier eventually reaches the point at which the loss term $-\alpha I_t$, which was neglected initially, is comparable to the saturated gain term. If losses are included, the intensity is governed by

$$\frac{dI_t}{dz} = \frac{kI_t}{\sqrt{\pi}\epsilon(1 + sI_t)} - \alpha I_t = 0, \quad (28)$$

which for $sI_t \gg 1$ has the steady-state solution

$$I_t = \frac{k}{\sqrt{\pi}\epsilon \alpha s} \quad (29)$$

These results may be collected as

$$I_t = \begin{cases} I_{t0} \exp\left[\frac{kz}{\sqrt{\pi}\epsilon}\right] & \text{lossless unsaturated regime} \\ I_{t0} + \frac{kz}{\sqrt{\pi}\epsilon s} & \text{lossless saturated regime} \\ \frac{k}{\sqrt{\pi}\epsilon \alpha s} & \text{loss-limited saturated regime.} \end{cases} \quad (30)$$

They are similar to Rigrod's solutions [9] for monochromatic radiation at gain center.

Using (24) and (30), (23) may be written for large distances as

$$\frac{\Delta\nu_{\text{hom}}}{\Delta\nu_A} = \begin{cases} \sqrt{\frac{\sqrt{\pi}\epsilon}{kz} \ln 2} & \text{lossless unsaturated regime} \\ \sqrt{\frac{\ln 2}{kz} \frac{1}{\sqrt{\pi}\epsilon}} & \text{lossless saturated regime} \\ \sqrt{\frac{\ln 2}{\alpha z}} & \text{loss-limited saturated regime.} \end{cases} \quad (31)$$

These results are valid provided that the spectrum is much narrower than the homogeneous line width before saturation sets in. As the gain is pulled down by saturation, the narrowing rate is slowed. When losses become important, the gain curve is clamped and the narrowing speeds up again. In a homogeneously broadened amplifier neither saturation nor losses stop the narrowing process. In Fig. 1 are some numerical solutions for the line width of the emission from a homogeneously broadened superradiant laser amplifier as a function of the normalized distance $Z_{\text{hom}} = kz/(\sqrt{\pi}\epsilon \ln 2)$. For simplicity losses are assumed to be negligible. The parameter in these plots is the product $\epsilon = s\eta$.

For an inhomogeneously broadened amplifier ($\epsilon \ll 1$) it will be assumed that the intensity is nearly uniform over a natural line width. Then the intensity spectrum may be removed from the denominator integral in (2) and the result simplifies to

$$\frac{1}{I(y_i)} \frac{dI(y_i)}{dz} = \frac{k \exp[-\epsilon^2 y_i^2]}{1 + \pi s I(y_i)}. \quad (32)$$

The spectral density $I(y_i)$ is found in the various regions from (32) in a manner essentially identical to the homogeneous case. The results are

$$I(y_i, z) = \begin{cases} I(y_i, 0) \exp[kz \exp[-\epsilon^2 y_i^2]] & \text{lossless unsaturated regime} \\ I(y_i, 0) + \frac{kz}{\pi s} \exp[-\epsilon^2 y_i^2] & \text{lossless saturated regime} \\ \frac{k}{\pi \alpha s} \exp[-\epsilon^2 y_i^2] & \text{loss-limited saturated regime} \end{cases} \quad (33)$$

and consequently the spectral width for large distances is

$$\frac{\Delta\nu_{\text{inhom}}}{\Delta\nu_D} = \begin{cases} \frac{1}{\sqrt{kz}} & \text{lossless unsaturated regime} \\ 1 & \text{lossless saturated regime} \\ 1 & \text{loss-limited saturated regime.} \end{cases} \quad (34)$$

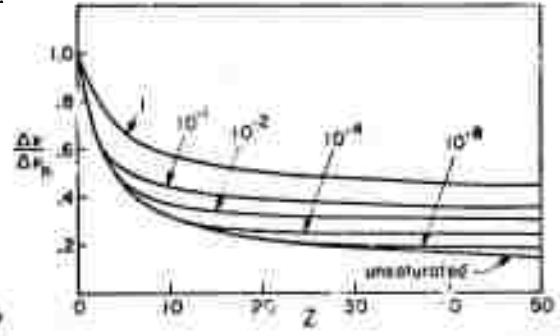


Fig. 1. Superradiant narrowing in a homogeneously broadened amplifier for various values of $\epsilon = s\eta$.

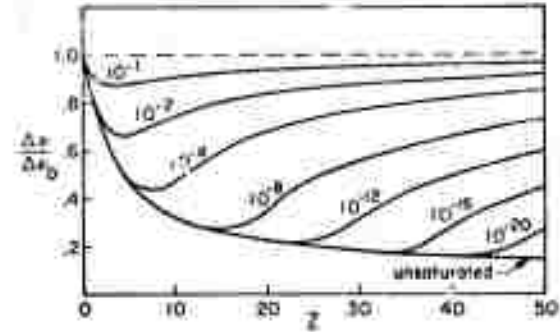


Fig. 2. Superradiant narrowing in a Doppler broadened amplifier for various values of $\epsilon = s\eta$.

It is evident that the effects of saturation on narrowing in an inhomogeneously broadened amplifier are significantly different from the effects in a homogeneously broadened amplifier. In the inhomogeneous case the onset of saturation reverses the narrowing process and restores the radiation to its Doppler line shape. This occurs because the center of the line saturates first, while the wings continue to grow exponentially. This analysis is valid provided that the intensity spectrum remains broad compared to the homogeneous line width. If the spectrum becomes narrow compared to $\Delta\nu_h$, the rebroadening would be expected to occur more slowly. Some numerical results for superradiant narrowing in an inhomogeneously broadened laser are shown in Fig. 2.

The minimum line width for a simple inhomogeneous superradiant source may be readily calculated. From (32) it is evident that saturation becomes important when $I(y_0) = 1/\pi s$. Then, using (5), one finds that saturation occurs at a distance z_{sat} given approximately by

$$g(0)z_{\text{sat}} = kz_{\text{sat}} = \ln \left(1 + \frac{1}{\pi s \eta} \right) \approx -\ln \pi s \eta. \quad (35)$$

Use of this expression in (12) yields the minimum line width

$$\Delta\nu_{\text{inhom min}} = \frac{\Delta\nu_D}{\sqrt{-\ln \pi s \eta}}. \quad (36)$$

Thus, if, for example, $\eta \approx 5 \times 10^{-6}$ W/m² and $s \approx 6 \times 10^{-9}$ m²/W in a xenon laser, then the Doppler line can be narrowed by at most a factor of about 5.5 before saturation becomes important at a distance (for $k \approx 15$) of about 2.0 m. These values for η and s are judged to be reasonably valid for a simple xenon laser used in some of our experiments based on the data of Clark [10]. This narrowing is not too impressive, and decreasing η by orders of magnitude does not help much, since the dependence on η involves a logarithm and a square root.

A possible scheme for reducing the ultimate line width is to place attenuators between sections of the amplifying medium [11]. These would cut down the intensity to prevent saturation without affecting the narrowing process. Even in such a system, however, the spectral line width could never approach zero because there is always broadband background noise being added to the beam by spontaneous emission. The result of the background is that the spectrum must eventually approach a narrow limiting line shape.

The narrowest possible line would be obtained in a long amplifier with distributed losses which are just sufficient to keep the line center intensity somewhat below the saturation intensity $1/\pi s$. To get an estimate of this limiting line shape one can write (3) for steady state with $I(y_0) = 1/\pi s$

$$0 = \frac{g_0}{\pi s} - \frac{\alpha}{\pi s} + \eta g_0. \quad (37)$$

Thus, the appropriate value for the loss constant α is

$$\alpha = g_0(1 + \pi s \eta). \quad (38)$$

Using this result, (3) away from line center can be written at steady state as

$$0 = g(y_1)I(y_1) - g_0(1 + \pi s \eta)I(y_1) + \eta g(y_1) \quad (39)$$

with the solution

$$I(y_1) = \frac{\eta g(y_1)}{g_0(1 + \pi s \eta) - g(y_1)} \approx \frac{\eta}{1 + \pi s \eta - \frac{g(y_1)}{g_0}}. \quad (40)$$

Keeping the second-order term in the power-series expansion of $g(y_1)$ leads finally to the intensity spectrum

$$I(y_1) = \frac{1/\pi s}{1 + (g_2/\pi s \eta g_0)y_1^2}. \quad (41)$$

Therefore, the narrowest possible line is a Lorentzian of width

$$\Delta\nu_{\min} = \Delta\nu_h \sqrt{\frac{\pi s \eta g_0}{g_2}}. \quad (42)$$

If the gain profile is the Gaussian given by (10) then $g_2 = g_0 \epsilon^2$ and the line width is simply

$$\Delta\nu_{\min} = \frac{\Delta\nu_h}{\epsilon} \sqrt{\pi s \eta} = \Delta\nu_D \sqrt{\frac{\pi s \eta}{\ln 2}}. \quad (43)$$

Using the approximate numbers given previously for s and η , one finds that the Doppler line would be narrowed by a factor of about 4×10^{-7} . A Doppler width of $\Delta\nu_D \approx 10^5$ Hz could yield an intensity spectrum of about 40-Hz width. If the oscillation frequency were about 10^{14} Hz as in xenon, the output could be used as an absolute frequency standard with a stability of about four parts in 10^{13} . Similar calculations can be carried out for the limiting line shape in a laser incorporating discrete rather than continuous losses.

The preceding discussion suggests that superradiant lasers could be useful as extremely stable frequency standards. Some practical limitations on such a system should be emphasized. The intensity only approaches its limiting form at a rate given by (12). Thus, to obtain a line width of 40 Hz for a gain constant of $k \approx 100$ m⁻¹ the overall length of the laser would have to be greater than 10^5 m. However, higher gain media are available and for some applications superradiant lasers should be useful as absolute frequency standards.

IV. EXPERIMENT

We describe here an experiment that has been performed in an effort to verify some of the conclusions of the previous sections regarding spectral narrowing. The apparatus used for this study consisted of a dc xenon discharge having an active region of 5.5 mm diameter and 1.1-m length. The xenon pressure was maintained at about 5 μ by means of a liquid nitrogen trap [12]. The laser was operated as a single mirror superradiant source.

To measure the width of the chopped superradiant output, we allowed it to impinge on an InAs junction detector. The resulting current was then fed into a conventional RF spectrum analyzer followed by a lock-in amplifier. It can be shown that under these conditions a Gaussian optical intensity spectrum $I(\xi)$ will give rise to a low frequency spectrum [13].

$$s(\nu) \propto \int_0^\infty I(\xi)I(\xi + \nu) d\xi, \quad (44)$$

which is also Gaussian and whose width is larger by $\sqrt{2}$ than that of $I(\xi)$.

A typical spectrum is shown in Fig. 3 for a current of 80 mA. This current corresponds to a gain of about $k \approx 12$ m⁻¹. The spectrum is approximately Gaussian in shape with a width of about 20 MHz. Therefore, the width of the original intensity spectrum is about 14 MHz.

The double-pass length of the laser amplifying medium is 2.2 m. Using (12), the intensity spectrum should be narrowed from the Doppler width by the factor $\sqrt{kz} = \sqrt{(12)(2.2)} = 5.14$. If the Doppler width were $\Delta\nu_D = 100$ MHz, then the intensity spectral width should be 19.5 MHz which is in satisfactory agreement with the measured width of 14 MHz. The discrepancy, if significant, could be due to a small amount of nonresonant feedback scattered back into the laser. Care was also necessary to



Fig. 3. Superradiant output spectrum for an 80-mA discharge current with 5-MHz/div dispersion.

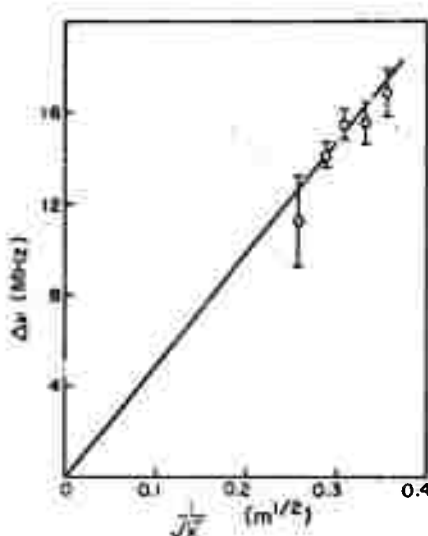


Fig. 4. Spectral width versus $k^{-1/2}$.

prevent resonant feedback, which could result, for example, from reflections off the detector. Resonant feedback led to longitudinal modes, which could be detected as periodic intensity fluctuations as the single mirror was scanned longitudinally.

Some experimental data are collected in Fig. 4. According to (12) the superradiant line width should be inversely proportional to the square root of the gain constant, which is in satisfactory agreement with the data. Line width data have not been obtained for lower values of gain because of the limited sensitivity of our detection system. At higher levels of gain the laser amplifier inevitably began to oscillate so that again meaningful data could not be obtained. These are only preliminary results and more refined experiments are in progress.

V. CONCLUSION

It has been shown in this paper that a gain profile which is quadratic in frequency near its maximum can support a narrowing Gaussian radiation spectrum. The

spectral width varies inversely as the square root of distance at long distances. In a homogeneously broadened amplifier saturation slows the narrowing process, while in an inhomogeneously broadened amplifier saturation restores the line to its original inhomogeneous line shape. Narrowed amplifiers are useful in spectroscopy, gain measurements, and anywhere a stable absolute frequency standard is needed.

Analogous results are obtained for laser oscillators if the coordinate z is replaced by the time coordinate ct/n_0 . One finds that the spectrum of an abruptly started laser oscillator should be a narrowing Gaussian that approaches ultimately a narrow limiting Lorentzian line because of spontaneous emission. The narrowing in this case results from the Fabry-Perot transmission resonances of the oscillator. Nonresonant oscillators operated near threshold may also be useful as frequency standards. Nonresonance can be obtained by making the cavity long so that the modes are closely spaced or by replacing one of the cavity mirrors with a scatterer [14].

REFERENCES

- [1] A. Yariv and R. C. C. Leite, "Super radiant narrowing in fluorescence radiation of inverted populations," *J. Appl. Phys.*, vol. 34, pp. 3410-3411, Nov. 1963.
- [2] G. Birnbaum, "Frequency stabilization of gas lasers," *Proc. IEEE*, vol. 55, pp. 1015-1026, June 1967.
- [3] E. I. Gordon, A. D. White, and J. D. Rigden, "Gain saturation at 3.39 Microns in the He-Ne maser," *Symp. Optical Masers*, Polytechnic Institute of Brooklyn, 1963, pp. 309-319.
- [4] A. Dienes, "Theory of nonlinear effects in a gas laser amplifier I. Weak signals," *Phys. Rev.*, vol. 174, pp. 400-414, sec. 3B, Oct. 1968.
- [5] J. W. Kliver, "Laser amplifier noise at 3.5 microns in helium-xenon," *J. Appl. Phys.*, vol. 37, pp. 2987-2999, July 1966.
- [6] L. W. Casperson and A. Yariv, "Gain and dispersion focusing in a high gain laser," *Appl. Opt.*, to be published.
- [7] J. H. Parks, D. Ramachandra Rao, and A. Javan, "A high-resolution study of the $C^3 \pi_u \rightarrow B^3 \pi_g (0, 0)$ stimulated transitions in N_2 ," *Appl. Phys. Lett.*, vol. 13, pp. 142-144, Aug. 1968.
- [8] D. F. Hotz, "Gain narrowing in a laser amplifier," *Appl. Opt.*, vol. 4, pp. 527-530, May 1965.
- [9] W. W. Rigrod, "Gain saturation and output power of optical masers," *J. Appl. Phys.*, vol. 34, pp. 2602-2609, Sept. 1963.
- [10] P. O. Clark, "Investigation of the operating characteristics of the 3.5 μ xenon laser," *IEEE J. Quantum Electron.*, vol. QE-1, pp. 109-113, June 1965.
- [11] E. I. Gordon, "Optical maser oscillators and noise," *Bell Syst. Tech. J.*, vol. 43, pp. 507-539, sec. 6, Jan. 1964.
- [12] D. R. Armstrong, "A method for the control of gas pressure in the xenon laser," *IEEE J. Quantum Electron.* (Corresp.), vol. QE-4, pp. 968-969, Nov. 1968.
- [13] A. T. Forrester, "Photoelectric mixing as a spectroscopic tool," *J. Opt. Soc. Am.*, vol. 51, pp. 253-259, Mar. 1961.
- [14] R. V. Ambartsumyan, N. G. Basov, P. G. Kryukov, and V. S. Letokhov, "Non-resonant feedback in lasers," in *Progress in Quantum Electronics*, vol. 1, pt. 3. New York: Pergamon, 1970, pp. 107-185.

MEASUREMENT OF THE RELATIVE NONLINEAR COEFFICIENTS OF KDP, RDP, RDA, AND LiIO_3 *

J. E. PEARSON **, G. A. EVANS and A. YARIV

California Institute of Technology, Pasadena, California 91109, USA

Received 14 December 1971

The nonlinear coefficients of RDP, RDA, and LiIO_3 have been measured relative to d_{36} of KDP using a cw ruby laser as a pump source. The new values found are $d_{36}(\text{RDP})/d_{36}(\text{KDP}) = 0.92 \pm 0.1$, $d_{36}(\text{RDA})/d_{36}(\text{KDP}) = 1.04 \pm 0.1$, $d_{15}(\text{LiIO}_3)/d_{36}(\text{KDP}) = 11.2 \pm 1.2$.

We wish to report the measurement of the nonlinear coefficients of RbH_2PO_4 (RDP), RbH_2AsO_4 (RDA) and LiIO_3 relative to d_{36} of KH_2PO_4 (KDP) [1]†. Previous measurements [2] of d_{36} of RDP and RDA used pulsed laser sources and thus are subject to a higher degree of uncertainty than measurements employing cw sources. The nonlinear coefficient of LiIO_3 has previously been measured to good accuracy [3] and was included in our measurements as a check on the accuracy of the experimental technique.

Our experimental setup employed a cw ruby as the fundamental light source. A schematic of the experimental arrangement is shown in fig. 1. The laser is similar to that described by Evtuhov and Neeland [4] and operated at an output power level of 100-200 mW. The output power was continuously monitored and an iris inside the cavity assured TEM₀₀ operation. The second harmonic power at 3472 Å was detected using a vacuum photodiode and standard lock-in amplifier techniques.

Because of the rapidly diverging output of our laser†† and in order to achieve easily observable UV outputs, it was convenient to focus tightly into the nonlinear crystals. Two different focal

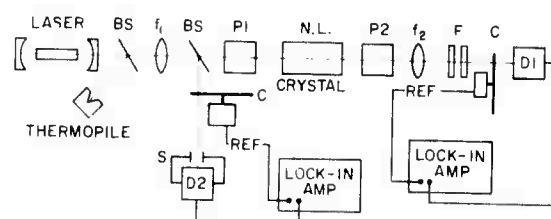


Fig. 1. Experimental arrangement for measuring relative second-harmonic powers and focused beam profiles. Laser: cw ruby; BS: beam splitter; f_1 : focusing lens; f_2 : collecting lens; P1 and P2: crossed polarizers; F: red-cut, UV-pass filters; C: chopper; S: 75 μ slit; D1: phototube with S-4 surface; D2: phototube with S-1 surface.

length lenses were used and the transverse profile of the focused beam scanned with detector-slit combination to obtain the confocal parameter in air†. The measured confocal parameters were then used with the measured relative UV powers and the focused-beam theory of Boyd and Kleinman [6] to obtain the nonlinear coefficients relative to $d_{36}(\text{KDP})$.

For KDP, RDP and RDA, all losses are assumed to be negligible at both 6943 Å and 3472 Å. The loss at 6943 Å in LiIO_3 is also neglected, but the crystal used in our measurements does have a finite absorption at 3472 Å. On the basis of measurements on a number of crystals [7], we have used $\alpha \approx 2 \text{ cm}^{-1}$ for the extraordinary second-harmonic wave in our LiIO_3 crystal.

† The confocal parameter of a propagating gaussian beam can be determined by measuring the spot radius at two points along the direction of propagation and applying the formulas of Pearson et al. [5].

* This work is supported in part by a grant from the General Dynamics Corporation and by the Advanced Research Projects Agency through the Army Research Office - Durham.

** Fannie and John Hertz Doctoral Fellow.

† $d_{36}(\text{KDP}) = (1.6 \pm 0.4) \times 10^{-9} \text{ esu}$.

†† The output confocal parameter of the laser was measured [5] to be $b = 2.3 \text{ cm}$ where $b = 2\pi\omega_0^2/\lambda$ and ω_0 is the minimum gaussian beam radius.

Table 1
Experimental values and relative nonlinear coefficients

Crystal	Phase matching angle	Crystal length (cm)	d	$d/d_{36}(\text{KDP})$	
				previous [ref.]	new value
KDP	51°	2.5	d_{36}	1.0	1.0
RDP	67°	1.8	d_{36}	1.04 ± 0.15 [2]	0.92 ± 0.1
RDA	90°	1.9	d_{36}	0.64 ± 0.15 [2]	1.04 ± 0.1
LiIO_3	52°	0.4	d_{15}	11 ± 1.5 [3]	11.2 ± 1.2

The results of our measurements are shown in table 1 along with previously reported values for the relative nonlinear coefficients. The values of $d_{36}(\text{KDP})$ for RDP and LiIO_3 agree with previous measurements to within the experimental error, but the value for RDA is 70% larger. All crystals were angle-tuned except RDA which was temperature-tuned. For our RDA crystal, manufactured by Quantum Technology, phase-matching at 90° to the optic axis occurred at a crystal temperature of 97.4°C and the second-harmonic versus temperature scan had a full-width at half-maximum of approximately 1.8°C .

The authors would like to express their indebtedness to Dr. Viktor Evtuhov for the loan of

the KDP, RDP, and LiIO_3 crystals and for his helpful comments and suggestions.

REFERENCES

- [1] J. E. Bjorkholm, IEEE J. Quantum Electron. QE-4 (1968) 970; Erratum QE-5 (1969) 260.
- [2] V. S. Suvorov, A. S. Sonin and I. S. Rez, Soviet Phys. JETP 26 (1968) 33.
- [3] F. R. Gabe, J. G. Bergman, G. D. Boyd and E. H. Turner, J. Appl. Phys. 40 (1969) 5201.
- [4] V. Evtuhov and J. K. Neeland, J. Appl. Phys. 38 (1967) 4051.
- [5] J. E. Pearson, T. C. McGill, S. Kurtin and A. Yariv, J. Opt. Soc. Am. 59 (1969) 1440.
- [6] G. D. Boyd and D. A. Kleinman, J. Appl. Phys. 39 (1968) 3597.
- [7] B. Soffer, private communication.

Sasson Somekh and Amnon Yariv

California Institute of Technology, Pasadena, California 91109

(Received 17 March 1972)

A proposal for a new method of phase matching in nonlinear optical interactions is made. A periodic perturbation of the surface of a thin-film waveguide generates space harmonics with new propagation constants which can be phase matched. An analysis of this proposal shows it to be particularly interesting for a class of thin-film nonlinear devices using the cubic optically isotropic semiconductors (such as GaAs, GaP, etc.) which possess high nonlinear optical coefficients but are not phase matchable by the conventional birefringent techniques.

Optically isotropic materials have, to date, not been used in nonlinear optical applications because the conventional technique of birefringent phase matching cannot be applied. This has, so far, precluded the use of many highly nonlinear materials, such as GaAs, from practical utilization in second-harmonic generation, parametric oscillation, and frequency upconversion.

One approach to phase matching in optically isotropic materials involves the use of dimensional dispersion in thin-film waveguides.¹ Another suggestion^{2,3} utilizes periodically laminated structures. The realization of this last approach involves a fractional wavelength control of the lamination period and has not yet been demonstrated.

As an outgrowth of our experiments on light guiding in epitaxial GaAs thin films,⁴ we have considered a new spatial modulation approach to phase matching, which involves a periodic corrugation of one (or more) of the boundaries of the thin-film waveguide, as shown in Fig. 1.

A more careful investigation of this idea leads to the conclusion that the expected magnitude of the effect, using presently available materials and techniques, is such as to encourage serious efforts to implement it. The main results of the analysis are presented in what follows.

Consider a single propagating mode, say m , in a thin (uncorrugated) waveguide with a principal transverse field component,

$$E_m^\omega(x, z, t) = C_m^\omega \exp[i(\omega t - \beta_m^\omega z)] \mathcal{E}_m^\omega(x), \quad (1)$$

in the presence of a sinusoidal boundary perturbation whose period Λ is large enough so as not to couple into the continuum ("leaky") modes⁵; the wave has the Floquet form

$$\begin{aligned} E_m^\omega(x, z, t) &= C_m(z) \exp[i(\omega t - \beta_m^\omega z)] \mathcal{E}_m^\omega(x) \\ &= \exp[i(\omega t - \beta_m^\omega z)] \mathcal{E}_m^\omega(x) \sum_{n=-\infty}^{\infty} A_{mn}^\omega \exp[-in(2\pi/\Lambda)z], \end{aligned} \quad (2)$$

where $C_m(z)$ is periodic in Λ . The mode consists of an infinite number of space harmonics, each with its phase constant

$$\beta_{mn}^\omega = \beta_m^\omega + n2\pi/\Lambda, \quad n = \pm 1, 2, \dots \quad (3)$$

Phase-matched interactions are thus no longer limited to the principal value of β but can involve the space harmonics. As an example, second-harmonic generation can be achieved by matching the fundamental ($n=0$)

space harmonic at ω to the first ($n=\pm 1$) space harmonic at 2ω , so that

$$\beta_0^\omega = 2\beta_0^{2\omega} \pm (2\pi/\Lambda). \quad (4)$$

The penalty for using the space harmonics is that the conversion efficiency is reduced relative to the phase-matched interaction in the bulk by a factor which in the example just quoted is approximately equal to $|A_{01}^{2\omega}|^2$. A meaningful evaluation of the feasibility of phase matching by periodic surface perturbation pre-requires a solution for the amplitudes of the space harmonics A_{mn} .

A solution of Maxwell's equations for a TE mode, to be described elsewhere, gives

$$\frac{\partial^2 C_m}{\partial z^2} - 2i\beta_m \frac{\partial C_m}{\partial z} = -k_0^2 C_m \int_{-\infty}^{\infty} |\mathcal{E}_m(x)|^2 \Delta n^2(x, z) dx, \quad (5)$$

where $\Delta n^2(x, z)$ is the deviation, due to surface corrugation, of the actual index (squared) of refraction from that of a planar boundary film. $k_0 = 2\pi/\lambda_0$ and $\mathcal{E}_m(x)$ is normalized according to $\int_{-\infty}^{\infty} |\mathcal{E}_m(x)|^2 dx = 1$. When a , the corrugation amplitude, is small compared to the thickness t , we can replace $\mathcal{E}_m(x)$ in Eq. (5) by $\mathcal{E}_m(0)$, and assuming $\partial^2 C_m / \partial z^2 \ll \beta_m \partial C_m / \partial z$, we obtain

$$C_m(z) = C_m(0) \exp \left\{ i \frac{k_0^2 |\mathcal{E}_m(0)|^2 (n_2^2 - 1) a \Lambda}{4\pi\beta_m} \left[\cos\left(\frac{2\pi}{\Lambda}z\right) - 1 \right] \right\}. \quad (6)$$

The corrugation thus causes a (spatial) phase modulation of the mode, so that, using Eq. (2) and a Bessel-func-

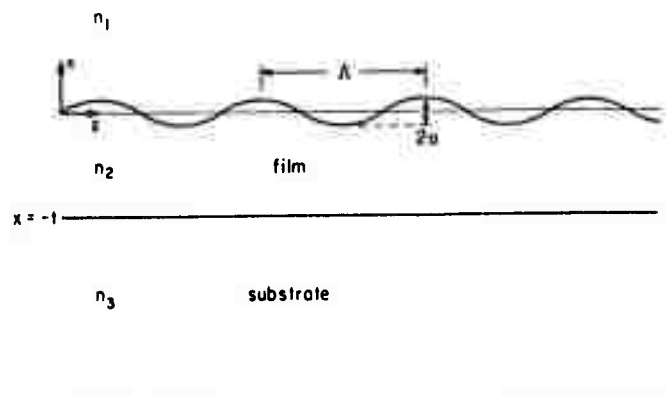


FIG. 1. Model of a thin-film waveguide with a periodic perturbation of one interface.

tion expansion of Eq. (6), we get the following solution for the mode:

$$E_m(x, z, t) = C_m(0) \exp[i(\omega t - \phi)] \mathcal{E}_m^\omega(x) \times \sum_{n=-\infty}^{\infty} (i)^n J_n(M_m) \exp\{-i[\beta_m^\omega - n(2\pi/\Lambda)]z\},$$

where

$$M_m^\omega \equiv \frac{k_0^2 |\mathcal{E}_m(0)|^2 (n_2^2 - 1) a \Lambda}{4\pi\beta_m} \quad (8)$$

Equation (7) gives explicitly the relative amplitudes of the space harmonics generated by the surface corrugation. This result can now be used in analyzing nonlinear interactions in a thin film. To be specific we consider an example of second-harmonic generation in which both the input (ω) and output (2ω) are in the same, say $m=0$, waveguide mode. We thus have

$$E_0^\omega(x, z, t) = \sum_n A_n \exp[i(\omega t - \beta_n^\omega)z] \mathcal{E}_0^\omega(x), \quad (9)$$

$$E_0^{2\omega}(x, z, t) = \sum_m B_m \exp[i(2\omega t - \beta_m^{2\omega})z] \mathcal{E}_0^{2\omega}(x),$$

where $\beta_n^\omega = \beta_0^\omega - n2\pi/\Lambda$, and A_n and B_m are defined by Eq. (7). The second-harmonic polarization generated by $\mathcal{E}_0(x, z, t)$ is taken as

$$p^{2\omega}(x, z, t) = d \sum_n \sum_i A_n A_i \exp[i\{2\omega t - (\beta_n^\omega + \beta_i^\omega)z\}] [\mathcal{E}_0^\omega(x)]^2, \quad (10)$$

where d is the appropriate bulk nonlinear tensor element. The rate of growth of the average power in the second-harmonic mode is

$$\begin{aligned} \frac{dP^{2\omega}}{dz} &= \omega W \operatorname{Im} \left(\int_{-\infty}^{\infty} E^{2\omega} (p^{2\omega})^* dx \right) \\ &= W \omega d \operatorname{Im} \left(\sum_n \sum_i \sum_m A_n^* A_i^* B_m \exp[i(\beta_n^\omega + \beta_i^\omega - \beta_m^{2\omega})z] \right. \\ &\quad \times \left. \int_{-\infty}^{\infty} [\mathcal{E}_0^\omega(x)]^2 \mathcal{E}_0^{2\omega}(x) dx \right), \end{aligned} \quad (11)$$

where W is the waveguide width in the y direction. Equation (11) shows immediately that a phase-matched interaction is due to triplets (n, l, m) or space harmonics for which the exponent in Eq. (11) vanishes, or, using Eq. (3), a phase-matched interaction occurs when

$$2\beta_0^\omega - \beta_0^{2\omega} + (n + l - m)(2\pi/\Lambda) = 0. \quad (12)$$

Phase matching in *first order* occurs if we choose the period Λ so that $2\beta_0^\omega - \beta_0^{2\omega} \pm 2\pi/\Lambda = 0$. The synchronous contributions, in this case, arise from the triplets $(0, 0, 1)$, $(0, -1, 0)$, and $(-1, 0, 0)$. A simple manipulation of Eq. (11) in which all non-phase-matched contributions are ignored, in which β is assumed to be equal to the bulk propagation vector, and where the energy is assumed to be confined mostly within the height t of the guide gives

$$\frac{P^{2\omega}(t)}{P^\omega} = \frac{2\omega^2 d_{eff}^2 t^2}{(n^\omega)^2 n^{2\omega}} \left(\frac{\mu_0}{\epsilon_0} \right)^{3/2} \frac{P^\omega}{Wt}, \quad (13)$$

in the nondepleted pump approximation. This result is of a form identical to the bulk interaction⁶ except that here the effective nonlinear coefficient is

$$d_{eff} \approx dJ_1(M_0^\omega). \quad (14)$$

The approximate equality is used since the exact numerical coefficient, which is of the order of magnitude of unity, involves the transverse overlap integral and the relative magnitude and sign of the three first-order contributions. It will be included in a more complete forthcoming paper.

The conversion efficiency from ω to 2ω is seen to be proportional to the mode power density P^ω/Wt . Since W and t can be made comparable to λ , this power density can become very large even for small power input. The penalty for using surface corrugation is a reduction of the effective nonlinear coefficient by the factor $\sim J_1(M_0^\omega)$. Using Eq. (8) in the case of a GaAs epitaxial film with $t=6 \mu$, $n_2=3.5$, and $n_2-n_3=0.2$, for a fundamental wave at $\lambda_0=10.6 \mu$ we find that first-order phase matching requires a corrugation with a period of $\Lambda=107 \mu$ and that, for $a=0.5 \mu$, $d_{eff} \approx \frac{1}{25} d_{GaAs}$. It is interesting to note that, even allowing for the $25\times$ reduction of the effective nonlinearity, using $d_{GaAs} \approx 1.2 \times 10^{-21}$ MKS, the effective coefficient is comparable to that of LiNbO_3 , one of the best phase-matchable materials presently used.

Note added in proof: Nonlinear interactions involving a spatial periodic modulation of the nonlinear coefficient d rather than the modulation of the height are also possible and will be discussed separately.

Experimental techniques for fabricating surface corrugations in GaAs with periods as small as 0.28μ have been developed in cooperation with Dr. H. Garvin of the Hughes Research Laboratories. The availability of such techniques plus the fast evolving technology of GaAlAs epitaxy should make possible the development of tunable optical parametric oscillators, upconverters, and second-harmonic generators using thin films.

*Work supported by the Office of Naval Research and by the Army Research Office, Durham, N.C.

¹D. B. Anderson and J. T. Boyd, Appl. Phys. Letters 19, 266 (1971).

²A. Ashkin and A. Yariv (unpublished).

³N. Bloembergen and A. J. Sievers, Appl. Phys. Letters 17, 483 (1970).

⁴D. Hall, A. Yariv, and E. Garmire, Appl. Phys. Letters 17, 127 (1970).

⁵D. Marcuse, Bell System Tech. J. 48, 3187 (1969).

⁶A. Yariv, *Introduction to Optical Electronics* (Holt, Rinehart and Winston, New York, 1971), p. 190.

Enhancement of self-focusing threshold in sapphire with elliptical beams*

C.R. Giuliano

Hughes Research Laboratories, Malibu, California 90265

J.H. Marburger

University of Southern California, Los Angeles, California 90007

A. Yariv

California Institute of Technology, Pasadena, California 91101

(Received 30 March 1972)

The power threshold for optically induced bulk damage in sapphire is a sensitive function of the ellipticity of the incident beam shape. Experimental results are consistent with a simple self-focusing theory.

We wish to report observations of the strong influence of departures from circularity of an optical beam on the power threshold for optically induced bulk damage in sapphire. This threshold, which is known to arise from the formation of a catastrophic self-focus in the medium,¹ is found to increase appreciably when the beam cross section is distorted from a circle to an ellipse, and when vertical and horizontal confocal parameters differ (leading to ellipsoidal phase fronts). These observations are consistent with the theoretical predictions of Vorob'yev² and Shvartsburg,³ which are extended slightly here to apply to our experiment.

Our experiments were performed using the output of a single-mode Q-switched ruby laser and amplifier focused inside sapphire samples with different lenses. The laser and associated monitoring apparatus are described in detail elsewhere.⁴ The far-field beam profile was measured to be Gaussian down to 8% of the peak, using a modified multiple-lens camera technique. Typical pulse lengths are 20 nsec. The sapphire samples are typically 3-in.-long by $\frac{1}{4}$ -in.-square bars.

Damage threshold powers for circular beams of different sizes are shown in Table I and compared with results for elliptical beams. The first three entries in Table I show the increased threshold power with beam size indicating the influence of electrostriction.¹ The dimensions listed in Table I are those at the beam waist, near which the self-focus first forms at threshold for circular beams. The remaining entries in Table I show the effect of noncircular beam shapes. The fourth entry gives the threshold power for an elliptical beam

whose short dimension is the same as the first entry, whose long dimension is the same as the third entry, and whose area is the same as the second entry. We see that the threshold power is appreciably higher for the elliptical beam compared with any of the circular beams. The last two entries in Table I show data for more elongated elliptical beams where we were unable to reach threshold at the maximum power available from our system.

Each power threshold in Table I was determined from a series of eight laser shots of differing peak powers. When damage occurred, the damaged region was found to possess a circular rather than an elliptical cross section. In fact, the appearance of the damage tracks formed above threshold was indistinguishable from those caused by circular beams. The tracks themselves were confined to the region between the two line foci of our astigmatic optical system, but there is no evidence that they would not extend beyond the upstream focus at higher powers.

To correlate these observations with theory, we have found it necessary to resort to the "paraxial-ray-constant-shape" analysis of self-focusing outlined in Ref. 5. More accurate numerical solutions of the nonlinear wave equation, such as those employed in Ref. 1, are extremely difficult to obtain in this case, because the noncircular beam shape requires an additional degree of freedom in the computer code. Nevertheless, the approximate analysis has had some qualitative success,⁶ and leads to simple expressions.

TABLE I. Comparison of damage threshold powers for circular and elliptical beams of different sizes.

Type of beam	Radius ^a (μm)	Area (μm ²)	Damage threshold power (MW)	Astigmatic focal length ^b in medium (cm)
Circular beams (dimensions at low-intensity waist)	14	6.3 × 10 ²	0.51 ± 0.04	...
	37	44 × 10 ²	0.74 ± 0.07	...
	100	308 × 10 ²	1.23 ± 0.10	...
Elliptical beams (dimensions at upstream low-intensity waist)	14 × 100	44 × 10 ²	6.0 ± 0.50	2.99
	14 × 1200	535 × 10 ²	> 17 ^c	∞
	7 × 1200	270 × 10 ²	> 17 ^c	∞

^aThe beam radius is defined as the 1/e radius for the intensity.

^bThis is the distance between the two line foci (see M. Born and E. Wolf, *Principles of Optics*, 3rd Ed. (Pergamon,

London, 1965), p. 171].

^cUnable to reach threshold at this power.

Assuming an optical field of the form

$$E = \frac{1}{2} E_0 \exp(i\varphi) \exp[i(kz - \omega t)] + \text{c. c.},$$

$$E_0 = E_m(z) \exp[-\frac{1}{2}(x^2/a^2 + y^2/b^2)],$$

we find by the method of Ref. 5 the following equations for the horizontal and vertical beam parameters a and b :

$$k^2 \frac{d^2 a}{dz^2} = \frac{1}{a^3} - \frac{\eta}{a^2 b}, \quad (1)$$

$$k^2 \frac{d^2 b}{dz^2} = \frac{1}{b^3} - \frac{\eta}{a b^2}. \quad (2)$$

Here $\eta = P/P_1$, where P is the total power and $P_1 = n^3 c / 4\epsilon_2 k^2$ in Gaussian units. The first terms on the right-hand sides of Eqs. (1) and (2) represent the effect of diffraction, while the second terms arise from the nonlinear contribution $\frac{1}{2}\epsilon_2 E_0^2$ to the dielectric constant. n is the linear refractive index. Vorob'yev,² who derived Eqs. (1) and (2) in a different way, has shown that they imply

$$\frac{d^3}{dz^3} (a^2 + b^2) = 0, \quad (3)$$

which can be integrated to give

$$k^2 (a^2 + b^2) = [k^2 (a_0^2 + b_0^2) + (2/a_0 b_0)(\eta_c - \eta)] z^2 + 2k^2 (a_0 \dot{a}_0 + b_0 \dot{b}_0) z + k^2 (a_0^2 + b_0^2). \quad (4)$$

Here a_0 and b_0 are the axes of the ellipse formed by the e^{-1} points of the transverse intensity profile at $z=0$, and $\eta_c = a_0/2b_0 + b_0/2a_0$. The initial rates of change \dot{a}_0 and \dot{b}_0 are simply related to the principal radii of curvature R_a and R_b of the phase fronts at $z=0$:

$$R_a = a_0/\dot{a}_0, \quad R_b = b_0/\dot{b}_0.$$

Using Eq. (4), the reader may easily find that the on-axis intensity, which is inversely proportional to $2ab \leq a^2 + b^2$, becomes infinite at the point

$$z_{f,m} = k a_0 b_0 (\eta/\eta_c - 1)^{-1/2}, \quad (5)$$

for plane incident phase fronts and $\eta > \eta_c$. It is therefore clear that the critical power for self-focusing is

$$P_c = \eta_c P_1 \quad (R_a = R_b = \infty), \quad (6)$$

which equals P_1 for circular beams. For finite values of R_a and R_b , a real solution for z of the condition $a^2 + b^2$

= 0 occurs only if P/P_1 exceeds

$$\eta_{cc} = \eta_c + \frac{(k a_0 b_0)^2}{4\eta_c} \left(\frac{1}{R_b} - \frac{1}{R_a} \right)^2. \quad (7)$$

For $P = \eta_{cc} P_1$, the self-focus occurs at $z = z_0$, where

$$-(a_0^2 + b_0^2)/z_0 = a_0^2/R_a + b_0^2/R_b. \quad (8)$$

For higher powers the self-focus will be found at

$$z_f = \frac{z_0}{1 + (z_0/k a_0 b_0)[(\eta - \eta_{cc})/\eta_c]^{1/2}}. \quad (9)$$

For the fourth entry in Table I, the beam parameters are $a_0 = 0.179$ mm, $b_0 = 0.232$ mm, $R_a = 4.05$ cm, and $R_b = 7.04$ cm. The measured power threshold for the onset of bulk damage was from five to twelve times higher than that for circular beams of comparable dimensions, and the damage first appeared at $z = 5.8$ cm from the entrance face. Assuming that the damage should first appear when a catastrophic self-focus forms at $P = \eta_{cc} P_1$, we expect from Eqs. (7) and (8) that the threshold power should be increased by $\eta_{cc} = 12.7$ and that the damage at threshold should appear at $z_0 = 5.51$ cm. The latter figure agrees well with the measured value, and the change in critical power is certainly of the right order. Unfortunately, our knowledge of the influence of the transient electrostrictive contribution to ϵ_2 is too poor to allow us to know which of the first three entries in Table I we should choose as P_1 . The first entry ($P_1 = 0.51$ MW) gives excellent agreement with theory, but the electrostrictive response for an elliptical beam can hardly be as large as that for a circular beam whose diameter equals the small radius of the ellipse. Nevertheless, the agreement with theory is sufficiently good to allow us to conclude that the damage morphology and threshold are well understood in terms of the self-focusing theory.

The theory outlined above gives simple formulas for the powers and distances at which the quantity $a^2 + b^2$ vanishes, but the intensity can become infinite only if the area πab of the beam vanishes. A closer examination of the solutions of Eqs. (1) and (2) shows that a and b both vanish at the same point. Prior to this point, the ratio a/b approaches unity. This is consistent with the observation that the cross sections of the damaged region have a circular shape along the entire length of the damage track. We remind the reader that at some point

- between the astigmatic line foci the low-intensity-beam cross section must be circular, but elsewhere it is elliptical

These results imply that difficulties which arise from bulk damage due to self-focusing in high-power optical systems can be avoided or ameliorated by the proper choice of beam parameters.

The authors are grateful to V. Evtuhov for helpful discussions and for providing English translations of Refs. 2 and 3.

*Work supported in part by the Advanced Research Projects Agency under ARPA Order No. 1434 with Air Force

Cambridge Research Laboratories.

¹C. Gullano and J. Marburger, Phys. Rev. Letters 27, 905 (1971).

²V. V. Vorob'yev, Izv. Vysshikh Uchebn. Zavedenii Radiofiz. 13, 1905 (1970).

³A. B. Shvartsburg in Ref. 2, p. 1775.

⁴C. R. Gullano and L. D. Hess in *Damage in Laser Materials*, Nat. Bur. Std. Special Publication No. 341, edited by A. J. Glass and A. H. Guenther (U.S. GPO, Washington, D.C., 1970), p. 76.

⁵W. G. Wagner, H. A. Haus, and J. Marburger, Phys. Rev. 175, 256 (1968).

⁶E. Dawes and J. Marburger, Phys. Rev. 179, 862 (1969). This paper contains a detailed comparison of results of the paraxial-ray-constant-shape approximation with exact numerical solutions.

MODES AND SPECTRA
OF
HIGH GAIN LASERS

Thesis by
Lee Wendel Casperson

In Partial Fulfillment of the Requirements
For the Degree of
Doctor of Philosophy

California Institute of Technology
Pasadena, California

1971